New Ridge Technologies

3600 Crondall Lane
Suite 110
Owings Mills, MD 21117

410-753-3055
hyaffe@newridgetech.com

Requirements for State of Polarization (SOP) Scrambling in Digital Equalizer and Transponder Verification

Henry Yaffe and Yaniv Barad
February 2011

I. Introduction

SOP scrambling and randomization are important elements in the development and performance verification digital-clock and data recovery chips (D-CDR) inside coherent Polarization-Multiplexed (PM) QPSK 40G and 100G systems. The Constant Modulus Algorithm (CMA), or variants thereupon, are among the most common digital signal processing equalizers implemented in D-CDRs due to the system requirement of blind estimation combined with practical chip limitations. However, one of the challenges for the CMA (or any other equalizer) is to minimize the convergence time of the algorithm when tracking a dynamically changing input signal.

The D-CDR equalizer's tasks are first to demultiplex the two orthogonal random and changing input polarizations, transforming them onto the linear X and Y axes of the receiver. Second, the D-CDR should remove transmission impairments in the optical transmission channel. Since changes in SOP changes the PMD signal degradation at the receiver, the D-CDR also needs to adapt to dynamic changes in PMD. For these reasons it is important to be cognizant of the rate of SOP changes that may occur in the network. In this white paper we shall review some of the measured network SOP changes published in the literature and discuss methods to synthesize SOP changes in the laboratory necessary to develop and verify D-CDR and transponder operation for reliable network deployment.

II. Review of Measured SOP changes in the Network

Changes in the signal SOP transmitted through a network has been measured.[1,2,3] In general, aerial fiber was found to change its SOP slower than 60 rad/sec while buried fiber was about an order of magnitude slower, as measurement histograms shown in the figure 1 below (copied from reference 1).

Faster SOP changes (<1ms) have been also been observed in the field[2,3] as well as artificially induced 'superfast' SOP changes caused by 'banging' a module of dispersion compensating fiber

---

[1] Peterson, Leo, Rochford, "Field Measurements of state of Polarization and PMD from a tier-1 Carrier", in Proc. OFC 2004, paper FI1.

[2] Boroditsky, Brodsky, Frigo, Magill, Rosenfeldt, "Polarization Dynamics in Installed Fiberoptic Systems," in Proc LEOS, 2005, paper TuCC1, p 414-415.

[3] Krummrich, Schmidt, Weishausen, Mattheus, "Field Trial on statistics of fast polarization changes in long haul WDM transmission systems," in Proc. OFC 2005, paper OThT6.

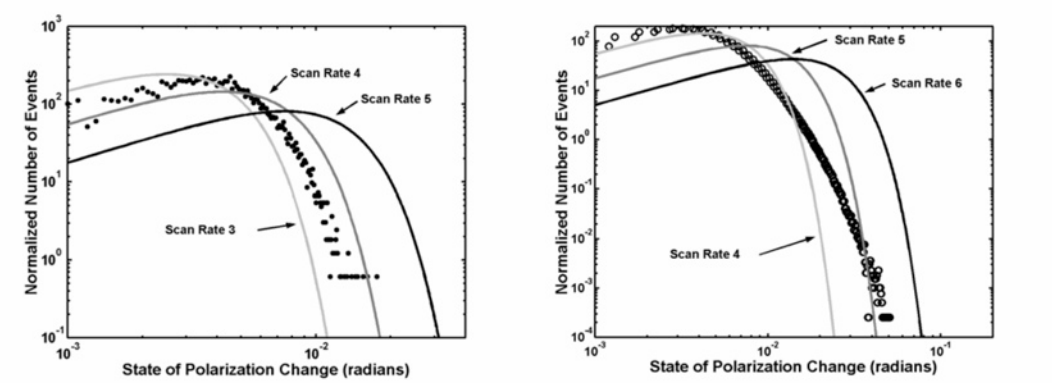

Fig 1: Histograms of SOP changes per ms in buried (left) and aerial (right) routes (shown in dots) relative to scan rates from an Agilent 11896A polarization controller (copied from reference 1).

(DCM).[4] In fact, the scariest data comes from reference 4. When a DCM was hit with a metal tool, 'superfast' SOP rotation rates of about 45,000 rotations/second (~280,000 rad/sec) were measured!

While we all expect central office craft are not walking around pounding DCMs with hammers, network elements can be hit and cover doors slammed closed. Nevertheless reference 4 has seriously tried to create a worse case scenario for extreme SOP change rates. Although this speed may be real, the probability of this ultra-fast SOP change event occurring is also extremely low. In fact during the long-term field measurements, fast, sudden, discontinuous/impulse SOP events were observed[2,3]. However, none of the observed SOP changes were as severe as in reference 4. In reference 2, about one fast SOP change event (~300 radians/sec) was observed per day. Even less frequently, reference 3, only observed three isolated SOP change events of greater than $\pi/10$ radians in ≤0.2ms (also ~300 radians/sec) in 2.5 months.

The conclusions drawn from this set of published data can be summed up by the following three SOP speed categories.

1. Per reference 1: SOP changes in fiber are in general continuous, with a distribution of rates up to about 60 rad/sec for aerial fiber and up to about 20 rad/sec for buried fiber.

2. Per references 2 and 3: fast events, ~300 rad/sec, are impulsive change in SOP occurring with a measured probability of ~2 x E-8 (i.e. ms/day)

3. Per reference 4: 'superfast' SOP change events, ~280,000 rad/sec, have been generated in extreme lab conditions, but have never been measured in the field. The probability of this type of event is even lower, and would likely only be induced by a severe physical disturbance to a network element rack.

Per references 2, 3 and 4: the fast and 'superfast' SOP speed events are not continuous rotations around the Poincaré sphere, but seem to be discontinuous SOP movements or 'bounces' of amplitude ~2π *radians or less.*

III. Testbed for SOP stress of D-CDRs and Transponders

The above types of SOP changes can affect (new 40G and 100G PM-QPSK) transponders and D-CDRs in two ways. First these SOP changes must be tracked by the digital polarization demultiplexer inside the D-CDR. Failure of the D-CDR to properly demultiplex would leave a

[4] Krummrich, Kotten, "Extremely fast (microsecond scale) polarization changes in high speed long haul WDM transmission systems", in Proc. OFC 2004, paper FI3.

mixed X and Y polarization state at each detector that could not be further processed, leading to bit errors. ***Therefore (even for a perfectly clean optical channel) the D-CDR chips need to be tested with dynamic SOP changes to verify the function of their polarization demultiplex function.*** Second, the D-CDR removes impairments from the optical channel. Polarization induced impairments such as PDL and PMD change as the SOP changes. The D-CDR often uses the CMA model to dynamically calculate and change the equalizer weights in order to track and remove these deleterious effects. **Hence testing the ability and the speed of the combination of SOP changes on PMD (and PDL) must also be part of D-CDR verification.**

Fig. 2: On the left is a view of a scrambled SOP displayed on the Poincaré sphere.

On the right is the subsequent optical tracking of the scrambled polarization to the desired SOP state.

The D-CDR must be able to digitally perform this function nearly flawlessly for the polarization demultiplex function at the input to the chip.

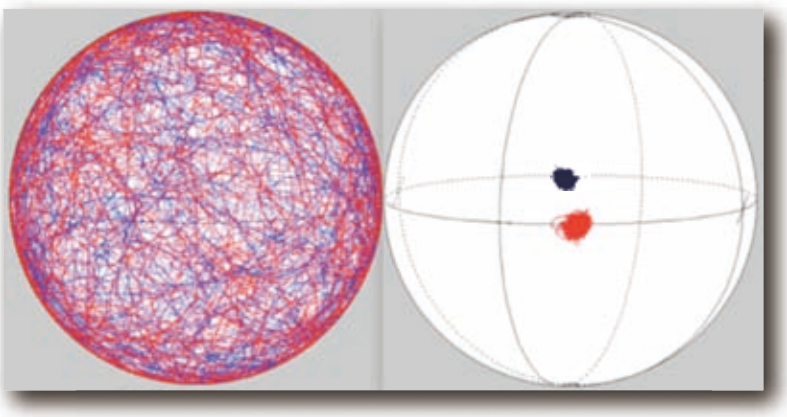

The goal of this paper is to identify how to vary the polarization to best test the capability of the D-CDR's algorithm to readjust itself to those SOP changes. Since we are considering the effects of polarization changes on both the polarization demultiplexing and the PMD mitigation capabilities of the D-CDR, two separate, and independently settable, polarization controllers are required. The generalized testbed shown in figure 3 is therefore recommended.

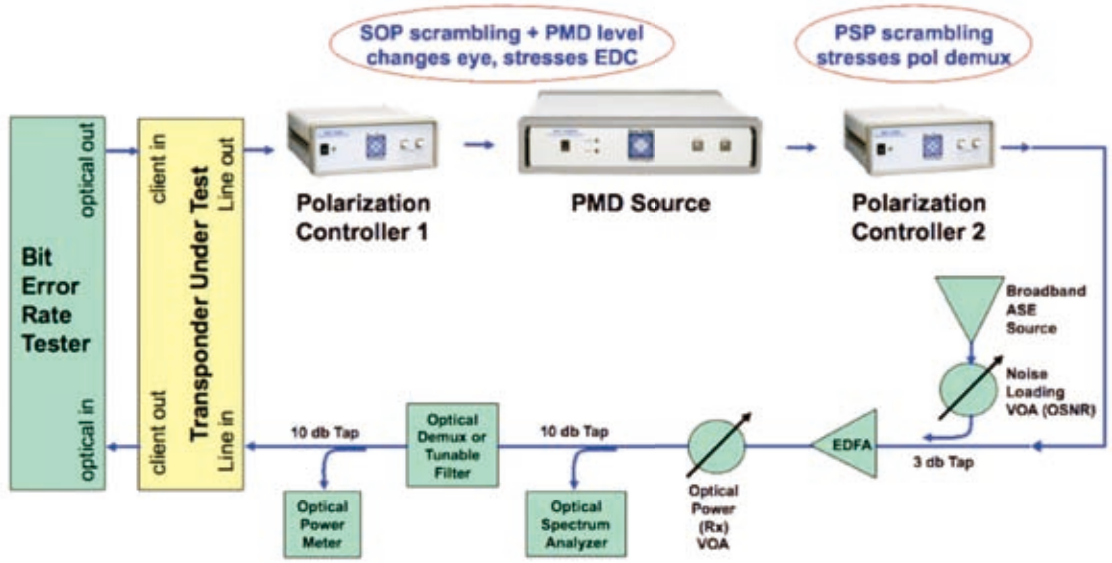

Fig. 3: Testbed set-up to develop and verify D-CDR capability to demultiplex the input polarization and mitigate PMD. Polarization Controller 1 and the PMD Source generate a dynamically randomized PMD state, while Polarization Controller 2 scrambles the polarization state 'seen' by the D-CDR polarization demultiplexer section. If only polarization demultiplexing is to be studied, Polarization Controller 1 and the PMD Source can be turned off or eliminated.

In the set-up in figure 3: the two scrambling sources employed to exercise the polarization demultiplexer and the PMD mitigation capabilities of the D-CDR are two distinct polarization control units. This is because physically there are two independent changes to the optical signal caused due to SOP changes. The first is simply the SOP presented to the receiver for polarization demultiplexing. This is the case if the fiber, within the central office, before the receiver were moved or rotated. The other is the effect of changes in the SOP that cause changes to the PMD distortion of the fiber link itself. In general the SOP can be rotated before the source of PMD, as in the central office of the transmitter, or the SOP could change somewhere mid-span.

If the SOP changes in between two PMD generating spans, the net PMD of the total line will change from (DGD_1, $SOPMD_1$) to (DGD_2, $SOPMD_2$). The weighing function of the equalizer to mitigate the the PMD state changes along the trajectory from (DGD_1, $SOPMD_1$) and (DGD_2, $SOPMD_2$). So the trajectory, and the transition time along the trajectory is the challenge for the equalizer algorithm, not necessarily the PMD of the endpoints. In fact, from the point of view of the D-CDR receiver, the endpoints are indistinguishable from any other point along the trajectory. For the D-CDR to work correctly it must be able to adjust its state as the PMD distortion changes from each (DGD, SOPMD) to (DGD+Δ, SOPMD+δ), regardless of the endpoints. The difficulty for the equalizer algorithm is therefore related to the length of the trajectory between these two PMD states. Testing all possible trajectories between all possible PMD state pairs, (DGD_1, $SOPMD_1$) to (DGD_2, $SOPMD_2$), is impractical if not impossible.

Moreover, imitating the PMD state transition from (DGD_1, $SOPMD_1$) to (DGD_2, $SOPMD_2$) by rotating the mode-mixers (i.e. polarization controllers in between the birefringent stages) inside a PMDS is not a well-defined, controlled or repeatable experiment. First, when the mode-mixers of the PMDS are changed, the PMD-trajectory between the two states is unknown for most PMD sources. Only with the New Ridge PMDS, running the PMD Randomizer (NRT-PMDR) are direct straight trajectories between randomized PMD states assured. For all other PMDSs, each rotated mode-mixer will contribute its own component trajectory to the total PMD state-to-state trajectory. In the lab test environment the state-to-state trajectory between the desired endpoints will change with time and generally will not be repeatable (for incoherent PMDSs); two PMDS units will not be create the same trajectories; and different PMDS models will not produce similar transitions. Second, and most importantly, the PMD states along the trajectory may pass through higher DGD and SOPMD levels than endpoints (as in the case of states (V,W) and (X, Y) in fig. 4) making PMD mitigation more difficult than for the endpoints you intended to evaluate. This leads to erroneous data and a waste of time. A better, well-defined, and more controllable experimental dynamic PMD test methodology is desirable.

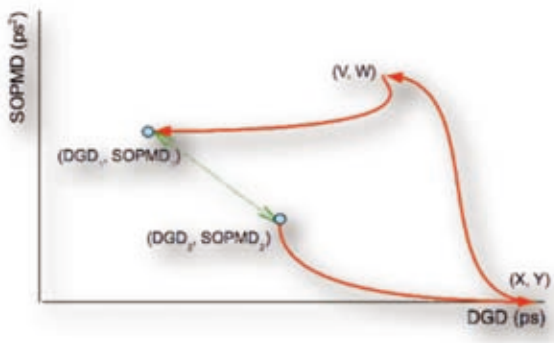

Fig 4: Scanning a PMDS from state (DGD_1, $SOPMD_1$) to (DGD_2, $SOPMD_2$) will (generally) not produce the intended (dashed-green) trajectory. Because each rotated mode-mixer will create a different trajectory path: e.g. moving 3 mode mixers may move (DGD_2, $SOPMD_2$) to (X, Y), then from (X, Y) to (V, W), and finally from (V, W) to (DGD_1, $SOPMD_1$) for the case shown at the left. Hence you are not testing the intended (DGD_1, $SOPMD_1$) to (DGD_2, $SOPMD_2$) transition, but actually testing the harder transition from states (V, W) to (X, Y). Moreover, these trajectories are usually not reproducible.

To solve the experimental difficulty described above, we recommend that the PMD mitigation capabilities of the D-CDR's equalizer be tested by dynamically ***scrambling the SOP input to the PMDS while keeping the PMDS state constant at (DGD_i, $SOPMD_i$)***. This may be counterintuitive at first. However, in scanning the input SOP we exploit the fact that when the SOP is aligned to the principal state of polarization (PSP) of the PMDS, its output DGD level is 0. Hence scrambling the input SOP is a systematic and controllable method to emulate the dynamic scanning the PMD from (DGD_i, $SOPMD_i$) to (0, ~0). Furthermore, for common equalizer

algorithms, such as CMA, the equalizer will not differentiate between the distortion change created rotating the input SOP to the PMDS and between changing state of the PMDS.

The input SOP rotation method is preferable for three practical laboratory test and measurement reasons:

1. rotating the input SOP to the PMDS is a more extreme test, as the trajectory from (DGD_i, $SOPMD_i$) to (0, ~0) is more taxing on the equalizer than the 'shorter' direct trajectory from (DGD_1, $SOPMD_1$) to (DGD_2, $SOPMD_2$);

2. states along all of the possible trajectories have lower PMD values than the endpoints, i.e. ($<DGD_i$, $<SOPMD_i$); and

3. this technique is a more convenient, systematic, consistent and repeatable methodology for testing the equalizer's PMD mitigation of dynamic state-to-state PMD transitions.

Therefore by placing a polarization scrambler before the PMDS (as in fig. 4), the generated eye pattern seen by the receiver will vary as if the PMD were dynamically changing between (0, ~0) and (DGD_i, $SOPMD_i$) (see fig. 6). This will stress the receiver's adaptive capability to readjust to dynamic PMD changes. In this manner the dynamic response of each PMD state set on the PMDS can be measured in a deterministic, repeatable and systematic fashion desirable for the development and verification of D-CDR based transponders.

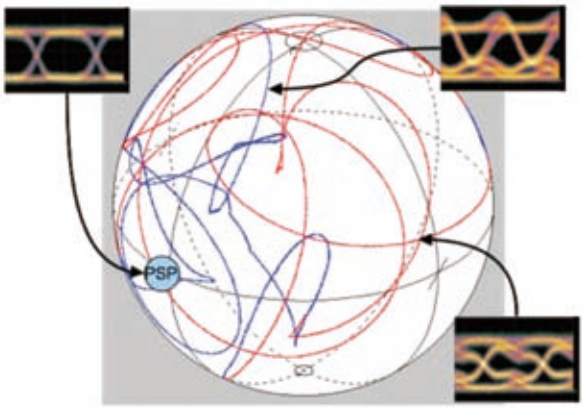

Fig. 5: For illustration, three eye patterns for a 10G NRZ signal are shown at the output of the PMDS fixed at (80, 3500). When the SOP is aligned to one of the PSPs of the PMDS, there is minimal PMD distortion and the state appears as (0, ~0). Because of the presence of both DGD and SOPMD distortions, the input SOP that challenges the equalizer mitigation algorithm the greatest is not known a priori.

Clearly changing the SOP before the PMDS dynamically changes the distortion presented to the D-CDR.

Fig. 6: Extending the above discussion, we can heuristically map the SOP rotations from the Poincaré sphere onto DGD-SOPMD space. When the SOP=PSP the state presented to the reciever is (0, ~0). As the SOP scans, the D-CDR received distortions follow various trajectories from (0, ~0) to (DGD_{set}, $SOPMD_{set}$) and back.

Scanning the SOP input to the PMDS is a controlable, systematic and very effective way to stress the transponder and D-CDR to dynamic PMD changes.

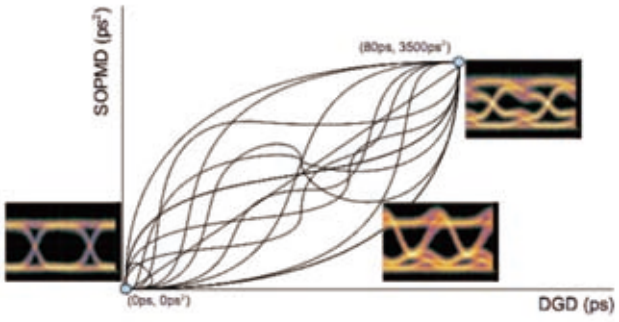

IV. Emulating Network-Like SOP changes in the Lab

Now that we understand (1) how the SOP changes in the network, and (2) how to set up a testbed to controllably reproduce these network behaviors, it is left to find an adequate

polarization controller to do the job. The statistics of polarization scramblers were first studied and verified by Leo, et. al.[5] who showed that random polarization scramblers are described by a Rayleigh statistics with distribution

$$D(r) = r/b * \exp(-r^2/2b),$$

where the maximum SOP deviation per interval of time, r, is defined by $r^2 = \theta^2 + \phi^2$, with θ the azimuth and ϕ the elevation angles on the Poincaré sphere. This distribution has only one fit parameter, b. It is much more quantitative and informative to describe the SOP generator by the frequency $b^{0.5}$ than the arbitrary 'scan rate' or the rotation rate of the fastest waveplate, because ***$b^{0.5}$* provides complete information about the SOP statistics.**

The peak of the Rayleigh distribution is given by

$$r_{peak} = b^{0.5}$$

and the mean SOP deviation,

$$\langle r \rangle = \sqrt{(\pi/2)} * r_{peak} \sim 1.25 * r_{peak}.$$

We define the maximum SOP

$$r_{max} \cong 3\langle r \rangle \sim 3.76 * r_{peak},$$

where *<0.1% of the SOP changes will be faster than r_{max}.*

Fig 7: Normalized Rayleigh Distribution

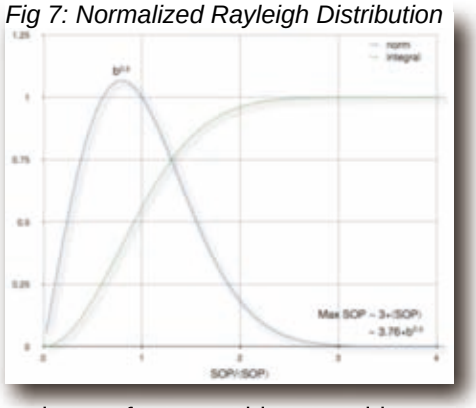

Leo, et. al.[5] also described a method of rotating the waveplates of a scrambler to achieve a Rayleigh distribution. The important point of this model is that the waveplates do not rotate at a constant speed, but are time varying. The instantaneous frequency of the nth waveplate is given by $F_n(t) = f_n \times Q_n(t)$, where, for example, the base frequency of each plate is f_n = *{f, 2*f, 3*f, 3*f, 7*f, 11*f,...}* and $Q_n(t)$ is a time dependent randomizing function ranging from 0 to 1. The Q_n term is vital to randomize the SOP in order to cover the entire Poincaré sphere. However the tradeoff is also clear. While the Q_n term provides complete and uniform coverage of the Poincaré sphere, it also lowers the average scrambling speed. Polarization controllers often advertise their fastest rotation speed, f_n^{max}. In general, the averaged rotation speed of the scrambler due to the combined movements of the cascaded waveplates' speeds, f_n, and their associated Q_n is much lower than f_n^{max}. **Therefore purchasing a polarization scrambler based on the speed of the fastest waveplate does not necessarily indicate the rotation speeds produced in an experiment.**

One of the most common fiber optic polarization scramblers is the (discontinued) HP 11896A, which uses, motorized fiber paddles. It was so common that engineers often qualitatively refer to the scrambling speed by its arbitrary 'scan rate' number 1 to 8. The 11896A is a random polarization scrambler. In the 11896A, each of the four fiber paddles is rotated at a different frequency, f_n. Since the four paddles rock back and forth, the paddle frequency varies in time by $Q_n(t)=\sin(f_n t)$. Therefore the instantaneous rotation frequency of the nth paddle is time dependent, $F_n(t) = f_n \times \sin(f_n t)$ *which ranges from* $0 \le F_n(t) \le f_n$.

We have compared the randomization of three scramblers in the following figure; the HP 11896A, the Adaptif A2000 (now sold as the Agilent N7784B) which uses a LN polcon and the NRT-2500, also using LN polcon. On the left of figure 8 is a picture of the SOP coverage of a Poincaré sphere by an HP 11896A at its maximum scan rate 8 showing a uniform distribution of SOPs. The middle picture is the result for the Adaptif A2000 (i.e. Agilent N7784B). It has a very fast LN polcon device and estimates its maximum instantaneous SOP scan speed to be 1237 rad/sec. However, the A2000 does not cover the Poincaré sphere uniformly, but tends to have preferred

[5] Leo, Gray, Simer, Rochford, "State of Polarization Changes: Classification and Measurement", Journal of Lightwave Technology, Vol, 21, #10, October 2003, pp 2189-2193.

SOP trajectories. ***The imperfect non-Rayleigh scrambling of the A2000 (i.e. Agilent N7784B) would therefore not be the best choice to use for testing the polarization demux or PMD mitigation function of and D-CDR.*** The picture on the right is the result for the NRT-2500. It combines the super-fast speed of the LN polcon with Q_n values randomly varying between 0 and 1 to complete cover the Poincaré sphere.

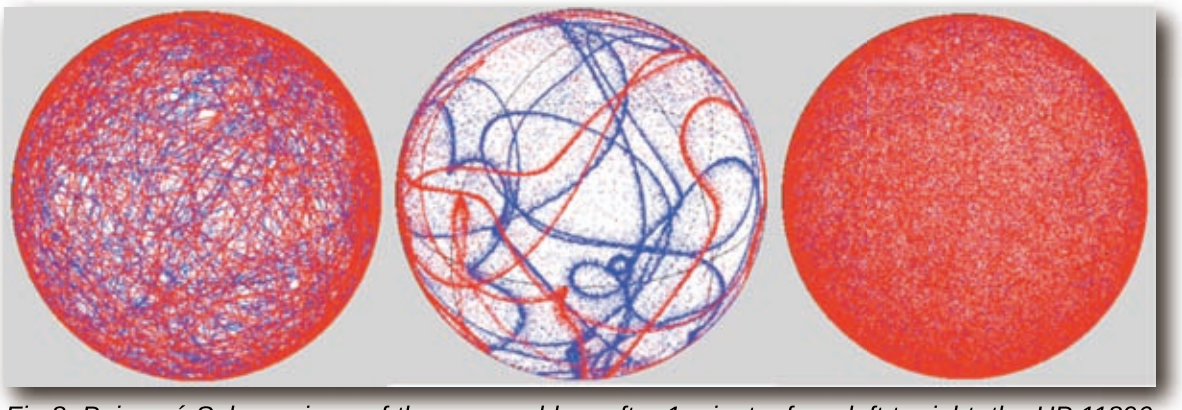

Fig 8: Poincaré Sphere views of three scramblers after 1 minute. from left to right: the HP 11896 using motorized fiber paddles, the Adaptif A2000 (now the Agilent N7784B) using LN polcon, and the NRT-2500 using LN polcon,. It is obvious that the Adaptif (i.e. Agilent) product does not completely randomize the polarization.

In figure 1 (copied from reference 1), the non-Rayleigh SOP distributions of aerial fiber and buried fiber were compared to the HP11896A. A Raleigh SOP distribution of r_{peak} = 14 rad/sec created using a HP11896A set to scan rate 6 had a broader SOP distribution than SOP distributions of either aerial and buried fiber. ***Therefore, any random SOP generator with a r_{max} ~ 55 radians/ sec is more than adequate to capture normal SOP changes in the network as described by SOP speed category #1 in section II. Specifically, the NRT-2500, set to scramble mode, can produce the necessary speed distribution, r_{max} = 64 radians/sec.***

In figure 9 the SOP variations of the three polarization scramblers, each set to their maximum scrambling speed setting, were measured, plotted and fit by Rayleigh distributions (per reference 5). The mechanical HP11896A fits the Rayleigh distribution very well, but was the slowest. For the unit we tested, scan rate 8 corresponded to r_{peak} =18 rad/sec. The A2000 was much faster. However, the A2000 does not uniformly cover the Poincaré sphere tending to follow preferred trajectories (fig. 8). This shows up as spikes on the SOP histogram and poorly fit by the Rayleigh distribution with r_{peak} =710 rad/sec, and is truncated above 2000 rad/sec. The NRT-2500 has much nicer fit to the Rayleigh distribution with r_{peak} =1940 rad/sec.

SOP speed category #2 in section II identifies infrequent fast network SOP rotation events, about 300 rad/sec in the network. ***The NRT-2500, set to r_{peak} ~ 300 rad/sec, would be sufficient to meet this target of SOP speed category #2 events.***

SOP speed category #3 in section II refer to ‘superfast’ artificially lab-induced SOP changes. The NRT-2500 has a second mode to generate such very rapid SOP changes, namely the Polarization Randomizer. In the Polarization Randomizer mode the angles of each of the waveplates are assigned random values at each time interval. This causes the SOP to slew from one SOP to another SOP at an extremely fast rate, limited only by the slew speed of the voltage drivers (~1 µsec). **Hence the maximum SOP scan rates for the NRT-2500 is greater than 1,000,000 rad/sec! The NRT-2500’s Randomizer mode can be adapted to emulate the types of extreme SOP jump discontinuities observed from bumping DCMs in *SOP speed category #3*.**

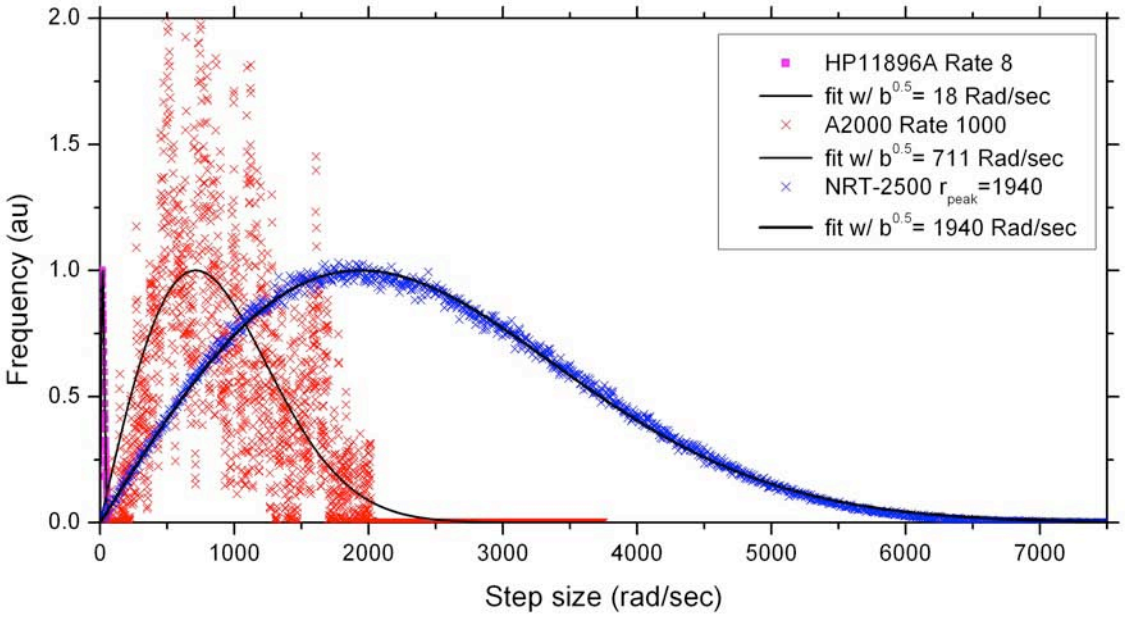

Scrambler Product	Polarization Control Technology	Speed settings	Poincaré sphere coverage	Fit $r_{peak} = b^{0.5}$ at max rate
HP11896A	**motorized LeFevre fiber paddles**	**8**	**Uniform**	**18 rad/sec** *(unit dependent)*
Adaptif A2000/ Agilent N7784B	**Integrated optic $LiNbO_3$**	**1000 linear scale**	**Non-uniform**	**711 rad/sec non-Rayleigh**
NRT-2500	**Integrated optic $LiNbO_3$**	**continuous, set r_{peak}**	**Uniform**	**1940 rad/sec**

Fig 9: Normalized histograms of the HP11896A, Adaptif A2000 and NRT-2500 at their fastest scrambling rate with their associated Rayleigh distribution fits. The HP11896A matches Rayleigh statistics but only reaches r_{peak} = 18 rad/sec. The Adaptif A2000 does not match the random Rayleigh statistics well. The poor attempted fit resulted in r_{peak} = 711 rad/sec. The NRT-2500 matches Rayleigh statistics and achieves the fastest SOP changes of all three polarization controllers with r_{peak} = 1940 rad/sec and r_{max} ~ 7,300 rad/sec. Above is also a table summarizing

Fig 10: The measured SOP transition from -S_1 to S_1 (blue osciloscope trace) produced by the NRT-2500 in Randomizer Mode. Light exiting the NRT-2500 was passed through a polarizer into a fast detector. The ocsilloscope trace therefore captured SOP rotations on the equator of the Poincaré sphere. The (nearly) π/2 radian SOP transition took 1 µsec, equivalent to approximately 1,500,000 rad/sec.

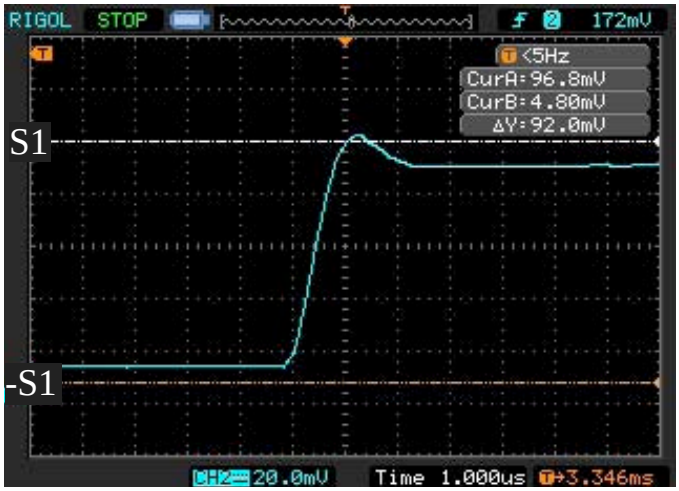

V. Summary and Conclusion

In the preceding white paper we have reviewed others' published measurements representative of SOP changes observed in the network and generated in the lab in our attempt to illuminate the necessary SOP and PMD speed specifications for testing and validating D-CDR algorithm performance. Specifying **a single polarization rotation rate does not capture physical processes observed in fiber network in terms of the spread of rotation frequencies, amplitude of rotation and probability of occurrence.**

Our goal here is to add to the discussion of the SOP change specifications and how to best generate them in the lab. Three SOP speed categories for D-CDR testing were identified from the literature corresponding to (1) normal buried and aerial fiber SOP changes that are less than 60 rad/sec; (2) fast, but isolated, SOP change events in the network about 300 rad/sec; and (3) 'superfast' SOP changes induced in the lab observed up to 280,000 rad/sec.

We pointed out that scrambling the SOP about the Poincaré sphere implies a distribution of frequencies. A truly random SOP scrambler has Rayleigh statistics described by one parameter, b, and having a distribution peak at $r_{peak} = b^{0.5}$. We defined a maximum SOP rotation rate, >99.9% of the SOP change events, to be $r_{max} \cong 3\langle r \rangle \sim 3.76 * r_{peak}$. It is important to remember that the maximum rotation speed of any waveplate in a polarization controller does not indicate the r_{peak} or r_{max} of the output SOP! Next we discussed how to recreate each of these three SOP speed categories in the lab in order to develop and verify the performance of D-CDR algorithms and transponders for network deployment. Of the measured polarization controllers, ***only the NRT-2500 was capable of meeting the requirements of all three SOP speed categories.*** Table 1 summarizes our conclusions.

SOP Speed Category	Target SOP Rate	NRT-2500 Mode	NRT-2500 Rate
1. regular buried & aerial fiber SOP variations	**r_{max} ≥20 & ≥60 rad/sec respectively**	**Scrambler**	**r_{max} = 64 rad/sec**
2. 'fast' impulsive SOP network events	**r_{peak} ~ 300 rad/sec**	**Scrambler**	**r_{peak} = 368 rad/sec**
3. 'superfast' lab-generated SOP changes	**2.8×10^5 rad/sec**	**Randomizer**	**slew = 5.6 µsec**

Table 1: Summary of the three types of SOP changes documented in the literature and controlled replication of these events in the laboratory with the NRT-2500 for D-CDR and transponder development and evaluation.

We also described the measurement testbed that would be required to develop and verify the capability of D-CDRs and transponders for polarization demultiplexing and PMD mitigation. ***Two independent polarization controllers are required for complete and accurate D-CDR testing***: one to scramble the SOP input into the PMDS generating the PMD dynamics (i.e. opening and closing the eye); and the second polarization scrambler, after the PMDS, stressing the polarization demultiplexer. When evaluating dual-polarization transponders, one polarization controller can only be used when there is no PMD source in the testbed.

Evaluating the measured scrambling speed of polarization controllers is complicated as incorrect test parameters can lead to dramatically different SOP change results. The detectors, A-to-D converters, data processing speeds and noise of commercial polarimeters dramatically influence the measured SOP change/interval histogram. For instance, if the polarimeter is too slow, it clearly cannot capture the large SOP swings, falsely weighing the data to slower SOP rates. More subtly, if the sampling interval is too long, then slower SOP changes are masked by the faster

ones occurring within the same interval. Conversely, if the sampling interval is too short, the fast SOP changes are truncated. Noise in the polarimeter detection/processing channel will be counted as small SOP changes within a measurement interval, appearing as excessive counts in the low frequency of the SOP histograms. Double checking your results is therefore recommended. For instance, measuring the -S1 to S1 changes by passing light though a polarizer to a fast detector and viewing the trace on an oscilloscope (as in fig 10.) is one good method to verify your testing. Another reliability self-check is that the Rayleigh fit, r_{peak}, should scale linearly with the measurement interval (as in table 1 in reference 5). Additionally, if the histogram is not well fit by a Rayleigh distribution, then either the scrambler is not random, or the polarimeter used in the measurement is inadequate or is set incorrectly.

During the writing of this white paper we have learned a lot of details about the nature of SOP changes and way to emulate them in the lab. We have some new ideas on improvements and modifications of the NRT-2500 Scrambler and Randomizer modes to make them even more useful for our customers. If you have any ideas or suggestions please contact us. (In fact this white paper was motivated by a customer question!) Our goal is to get the best product in the hands of our customers and your input is always highly appreciated.

We would like to thank Drs. Brian Heffner, Jens Rasmussen and Michael Taylor, all experts in the disciplines covered above, for their critical reading, comments and suggested improvements to this white paper.